JOURNAL OF SPACECRAFT AND ROCKETS
Vol. 31, No. 6, November–December 1994

Method of Filling Screen Liquid Acquisition Devices in Low Gravity

E. DiStefano* and E. C. Cady†
McDonnell Douglas Aerospace—West, Huntington Beach, California 92647
and
R. H. Rangel‡
University of California, Irvine, Irvine, California 92717

This work addresses the problem of filling screen-channel liquid acquisition devices in very low gravity. The concept of using a thermodynamic vent system to promote Clapeyron pumping and condensation is proposed in two configurations, a triangular apex-mounted heat exchanger and a concentric cylinder heat exchanger. The performance of the concept in low gravity is then evaluated by analysis. By approximating the liquid surfaces as flat and parallel, the triangular configuration is related to the cylindrical configuration. Results of a numerical solution to the one-dimensional cylindrical heat-transfer problem showed that a quasi-steady analytical solution suffices for the Jakob numbers of interest. For an initially empty, channel of 38-cm^2 cross-sectional area with a 10 : 1 ratio of channel height to heat exchanger radius, and 4-K Joule-Thomson expansion, complete fill occurs in 30 min. The concept was then proven by testing performed in 1*g* with Freon-114 at Jakob numbers similar to that in a hydrogen, on-orbit servicing environment. A screen-channel test article was successfully filled against gravity. This reliable method of filling screen channels enables on-orbit resupply of space-based systems that must deliver liquid in low gravity, such as a fuel depot.

Nomenclature

a	= cooling-tube radius, m
h_{fg}	= heat of vaporization, J/kg
Ja	= Jakob number, $c_p \Delta T / h_{fg}$ (dimensionless)
k	= thermal conductivity, W/m-K
P	= pressure, Pa
R	= bubble radius, m
r	= radial coordinate, m
R_g	= gas constant, J/kg-K
T	= temperature, K
t	= time, s
u	= radial velocity, m/s
Y	= dimensionless surface-tension-driven vapor-bubble collapse parameter
α	= thermal diffusivity, m^2/s
γ	= nondimensional condensate surface location, $r_s(t)/a$
ΔT	= $T_\infty - T_w$, K
ΔP	= $P_\infty - P_v$, Pa
ζ	= nondimensional radial coordinate, $(r-a)/[r_s(\tau)-a]$
η	= nondimensional radial coordinate, r/a
θ	= nondimensional temperature, $(T-T_c)/(T_{sat}-T_c)$
ρ	= density, kg/m^3
σ	= surface tension, N/m
τ	= nondimensional time, $Ja\,\alpha t/a^2$

Superscripts

(ν)	= at old time
$(\nu+1)$	= at new time
.	= first time derivative
..	= second time derivative

Subscripts

a	= cooling-tube radius
b	= at (of) bulk-liquid surface
c	= at cooling-tube surface
f	= final (at end of collapse)
l	= liquid
N	= last node
n	= nth node
q.s.	= quasi-steady result
s	= at (of) condensate surface
sat	= saturation
v	= vapor
w	= at bubble wall
0	= initial value
1	= first node
∞	= at infinity

Introduction

ON-ORBIT servicing and future space logistical operations will include the filling (and refilling) of tanks with cryogenic liquids. Many of these tanks must deliver liquid under low-gravity conditions and will likely use a screen-channel liquid acquisition device (LAD). The designs for screen LADs are commonly conduits, with walls made of porous, fine-mesh screen, that are routed around the perimeter of a tank and manifolded at the tank outlet. In order for these screen LADs to function properly, they must be full of liquid. However, there are several scenarios in which a screen device is left on orbit with vapor inside it, e.g., when a tank is launched dry, or when a heat leak vaporizes liquid inside the device, or when the screen has failed because of excessive outflow conditions. Consequently, a means of reliably filling LADs must accompany on-orbit tank fill and refill operations.

Presented as Paper 91-3540 at the AIAA/NASA/OAI Conference on Advanced SEI Technologies, Cleveland, OH, Sept. 4–6, 1991; received Dec. 2, 1993; revision received Feb. 23, 1994; accepted for publication March 30, 1994.

*Engineer/Scientist-Specialist, Mechanical/Propulsion/Thermodynamic Technology, Space Transportation Division, Mail Code A3-L260-46S-2, 5301 Bolsa Avenue. Member AIAA.

†Senior Manager, Advanced Propulsion, Space Transportation Division, 5301 Bolsa Avenue. Associate Fellow AIAA.

‡Associate Professor, Department of Mechanical and Aerospace Engineering. Senior Member AIAA.

Table 1 Reference environment

	Environment	Baseline condition
Orbit	Acceleration	$10^{-7}g$ (axial)
Fluid	Liquid hydrogen	Liquid hydrogen at 1.01×10^5 Pa
Tank	Shape	Spherical
	Volume	14.1 m^3
	Length	3.0 m
	Diameter	3.0 m
Thermal	Tank heat leak	0.1 W/m^2
Screen Liquid Acquisition Device	Nominal volume	2% tank volume
	Cross section	Triangular
	Width	10 cm
	Height	7.5 cm
	Length	4.7 m
	Wall thickness	1.52 mm
	Channel-to-wall gap	1.5 cm
	Screen	200 × 1400 twilled double Dutch weave (15-μm equivalent pore diameter)
Operations	Time for fill	< 2 h

An environment representative of on-orbit servicing, and thus of filling of screen LADs, is summarized in Table 1. It is characterized by liquid hydrogen in a well-insulated, pressurized tank, in very low gravity. Very low gravity is the most demanding condition. On the ground, a screen device can be filled by filling the tank, opening a vent at the top of the channel, and allowing buoyancy to displace gas in the channel from the bottom up. However, in low gravity, buoyancy tends not to be a significant displacement force. Whether liquid is fed into the tank outside of the channel or directly into the channel, it will tend to wet the walls of the channel and so is just as likely, if not more likely, to find its way toward a vent, thereby trapping gas inside the channel. Consequently, any attempt to continue venting will likely result in dumping of costly liquid overboard and may never result in fill of the LAD.

One approach that has been proposed for filling screen devices on orbit is the use of tapered flow paths.[1] Unfortunately, the reliability of this approach has not been substantiated. Another approach is to supplement resupply operations with a liquid-vapor separator. However, low-gravity liquid-vapor separation, particularly of cryogenic fluids, is not well developed. An alternative to trying to remove bubbles from the channel, as is attempted in the above approaches, is to collapse the vapor inside the channel.[1] This alternative is limited to the case where the gas is the pure vapor of the liquid; i.e., there are no noncondensible gases (e.g., helium pressurant). In the following sections, several modes of vapor collapse are reviewed, a promising concept is then proposed, the performance in low gravity is analyzed, and finally, $1g$ testing for proof of the concept is summarized.

Fill of LADs by Vapor Collapse

Spontaneous Collapse

Even under saturated conditions, surface tension establishes a pressure difference, and thus also a temperature difference, across the wall of a vapor bubble; consequently, there is a potential for the vapor to collapse spontaneously. To facilitate considering the spontaneous collapse of vapor inside a LAD channel, the channel is neglected and the vapor is assumed to be a spherical stationary bubble, alone in an infinite bath of incompressible, constant-property liquid saturated at the ullage pressure of the tank. Two processes must occur for the bubble to collapse: 1) the vapor must condense by the transfer of heat away from the bubble, and 2) liquid must overcome inertia to move to displace the condensed vapor. The rate of collapse is limited (controlled) by the slower of the two processes.

Consider the extreme case in which heat transfer controls the rate of collapse. The collapse rate is assumed small enough that the temperature gradient is never far from its steady-state value, i.e., conditions are quasi-steady. The energy balance across a spherical vapor-bubble wall is then

$$k_l \frac{dT}{dr}\bigg|_w = -\rho_v h_{fg} \frac{dR}{dt} \tag{1}$$

Evaluating conduction in the liquid in spherical coordinates, we have

$$\frac{1}{r^2}\frac{d}{dr}\left(r^2 \frac{dT}{dr}\right) = 0 \tag{2}$$

With thermodynamic equilibrium at the bubble wall and the temperature at infinity constant, conduction at the bubble wall is

$$\frac{dT}{dr}\bigg|_w \equiv \frac{\Delta T}{R} \tag{3}$$

which reduces Eq. (1) to

$$k_l \frac{\Delta T}{R} = \rho_v h_{fg} \frac{dR}{dt} \tag{4}$$

The saturation temperature in terms of the saturation pressure is obtained from the Clausius-Clapeyron relation[2]; for small temperature differences,

$$\Delta T_{sat} = \frac{\Delta P_{sat}}{h_{fg} P_{sat}/R_g T_{sat}^2} \tag{5}$$

The pressure difference across the bubble wall (with uniform pressure in the liquid phase) is obtained from the Laplace relation for a spherical bubble,

$$\Delta P = -2\sigma/R \tag{6}$$

Substituting Eq. (6) into Eq. (5) for ΔP_{sat}, and then the result into Eq. (4), the rate of collapse is

$$\left(\frac{dR}{dt}\right)_{\text{heat transfer}} = \frac{-2\sigma k_l T_{sat}}{(\rho_v h_{fg})^2 R^2} \tag{7}$$

Consider next the extreme case in which inertia controls the rate of collapse. Heat transfer is sufficient that the local liquid temperature, and thus the vapor pressure, does not rise enough to counter the inertia of the liquid. Only the momentum equation must be solved; for ideal flow in spherical coordinates, the momentum equation in the liquid phase simplifies to the Rayleigh equation[3]

$$R\ddot{R} + 3\dot{R}^2/2 = \Delta P/\rho_l \tag{8}$$

Assuming quasi-steady-state conditions, neglecting the local acceleration term, and substituting Eq. (6) into Eq. (8), the rate of collapse is

$$\left(\frac{dR}{dt}\right)_{\text{inertia}} = -\left(\frac{4\sigma}{3R\rho_l}\right)^{\frac{1}{2}} \tag{9}$$

Whether heat transfer or inertia controls the rate of spontaneous collapse can then be evaluated by the order of magnitude of the ratio of the rates of collapse found for the two extreme cases,

$$Y \equiv \left(\frac{dR}{dt}\right)_{\text{inertia}} \Big/ \left(\frac{dR}{dt}\right)_{\text{heat transfer}} = \frac{(4\sigma/3R\rho_l)^{\frac{1}{2}}}{2\sigma k_l T_{sat}/(\rho_v h_{fg})^2 R^2} \tag{10a}$$

$$Y \begin{cases} \ll 1, & \text{collapse controlled by inertia} \\ \approx 1, & \text{collapse controlled by both} \\ \gg 1, & \text{collapse controlled by heat transfer} \end{cases} \tag{10b}$$

For a vapor bubble with a diameter (6.9 cm) corresponding to the channel cross-sectional area and the conditions in Table 1, Y is on the order of 10^{12}; thus, the spontaneous process is controlled by heat

transfer. Integration of Eq. (7) provides the corresponding time for collapse,

$$t_f = (\rho_v h_{fg})^2 R_0^3 / 6\sigma k_l T_{sat} \tag{11}$$

The calculated time is 10^9 s, which suggests that the spontaneous collapse process is extremely slow (if possible at all).

Collapse by Ullage Pressurization

The extreme weakness of the process of spontaneous collapse (as revealed above) in the baseline environment is due in part to the extremely low driving pressure difference associated with the surface tension of the vapor bubble. One might try to enhance the driving pressure difference by simply pressurizing the ullage of the tank. Collapse is consequently induced in a subcooled, rather than saturated, liquid. A parameter that characterizes the mechanisms for vapor collapse under these conditions was identified in Ref. 3. Using this parameter for a pressurization, from 1 atm (saturated) to 2 atm, of the same vapor bubble (6.9-cm diameter) trapped inside the channel under the conditions of Table 1, collapse was found to still be controlled by heat transfer.[4] An analytical solution to the heat-transfer problem was developed in Ref. 5, which in terms of bubble collapse time is[3]

$$t = \frac{4}{3\pi} \frac{R_0^2}{\alpha_l Ja^2} \left(\frac{2}{R/R_0} + \left(\frac{R}{R_0} \right)^2 - 3 \right) \tag{12}$$

The time it takes for the bubble to collapse even to only half its original size is on the order of 2.5 h. Given such long collapse times, if the ullage is near the trapped bubble, the liquid will likely warm before full vapor-bubble collapse, thereby negating any superheat and, thus, any further collapse.

Proposed Concept: Thermodynamic Vent System (TVS) Heat Exchanger

From the above discussion, it is clear that collapse of vapor bubbles in the environment of Table 1 is heat-transfer controlled. It is a natural step now to speeding the sluggish heat-transfer process by using a heat exchanger. One type of heat exchanger, already known for use on tanks for long-term storage in space, is the thermodynamic vent system (TVS). The application of a TVS to a screen-channel LAD was originally introduced in Ref. 1. The concept is illustrated schematically in Fig 1. The heat exchanger uses the bulk fluid of the tank and immediately expands it through a Joule-Thomson device. This expanded fluid cools the tube, causing condensation of the saturated vapor in the channel and consequential displacement of condensing vapors by bulk liquid moving in through the screen wall of the channel. The expanding fluid exits the tank and is vented overboard.

The cooler surface of the TVS tube corresponds to a lower local saturation pressure and thus establishes a pressure difference between the bulk-liquid surface and the vapor in the channel. This pressure difference pushes the bulk liquid into the channel, a process referred to as Clapeyron pumping in its application to priming heat pipes.[6] However, the controlling factor in the rate of fill of the screen channel remains the condensation process itself. Because the vapor bubble cannot be vented, it must be condensed before liquid can move in and displace it.

In order for effective fill to take place, the screen surface of the channel must be completely wetted (sealed) by liquid on its exterior side. If the screen is not completely wetted, vapor from the ullage will move in (instead of bulk liquid) to displace the condensing vapor inside the channel. In low gravity, the fully wetted condition can be readily achieved by filling the tank first; the wetting and low Bond number of hydrogen in the orbital environment will insure wetting of the channels that are positioned along the tank wall. Additionally, the screens used by the channels encourage wicking along the screen length, and liquid inside or outside of the channel will tend to wick along the length of the channel, eventually resulting in a condition called "wickover" in which the entire screen is wetted by liquid wicked along the screen.[7]

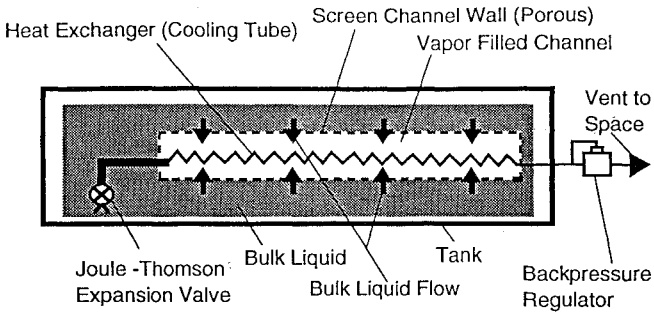

Fig. 1 Proposed concept: TVS heat exchanger to condense vapor along the length of the channel.

Low-Gravity Performance Analysis

Two configurations of the concept are analyzed to evaluate the time it takes to fill the screen LADs in low gravity: a concentric cooling tube and channel, and an apex-mounted cooling tube in a triangular channel. The concentric heat-exchanger configuration is addressed first because it is more amenable to analysis; moreover, it is promising as a design. The analysis for the concentric configuration is then applied in an approximate manner to the apex-mounted triangular configuration.

The concentric heat-exchanger configuration is illustrated in Fig 2. The bulk liquid supply of the tank completely surrounds the screen LAD channel. The wall of the channel is all porous screen. As liquid condenses on the cooling tube of the TVS, liquid moves in through the screen wall to displace the condensing vapor. The process is axially symmetric in very low gravity, as surface tension is dominant and the liquid hydrogen will tend to wet the surfaces uniformly.

Only hydrogen is present in the tank. Initially the temperature is uniform throughout at the saturation temperature corresponding to the tank ullage pressure. The bulk liquid inside the tank is assumed to be large in comparison with the total mass flow through the cooling tube. Consequently the decrease in density of the tank contents is very small, and the equilibrium pressure of the tank will remain approximately constant. The corresponding temperature of the vapor is then assumed to be constant at its original saturation value. Upon start of flow through the cooling tube, the temperature at the tube outer wall surface remains constant.

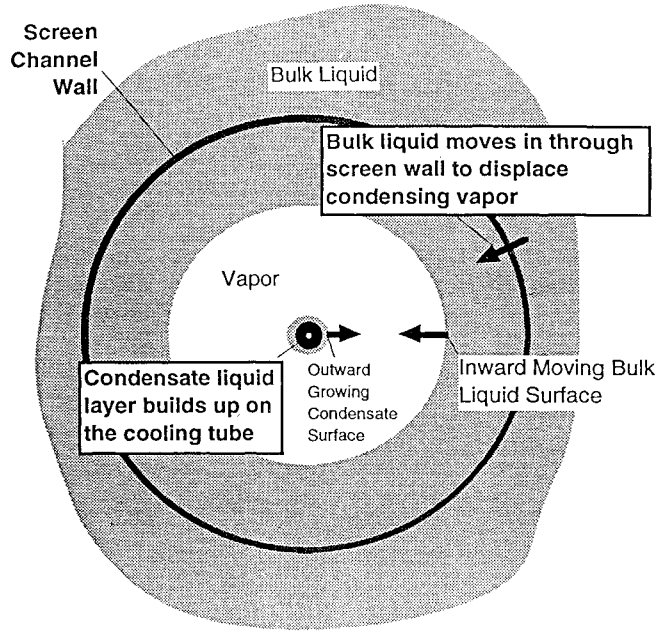

Fig. 2 Physical model of concentric heat-exchanger configuration.

The continuity equation for axial symmetry and constant properties in the liquid phase about the cooling tube is

$$\frac{1}{r}\frac{\partial(ru)}{\partial r} = 0 \tag{13}$$

which upon integration reduces to $ru = \text{const}$. The velocity at the cooling tube wall is zero; therefore the continuity equation reduces to zero velocity in the liquid condensate layer.

Because there is no motion in the liquid, the momentum equation is trivial and the remaining basic equation is the energy equation, which simplifies to the one-dimensional heat-conduction equation in cylindrical coordinates:

$$\frac{\partial T}{\partial t} = \frac{\alpha}{r}\frac{\partial T}{\partial r} + \alpha\frac{\partial^2 T}{\partial r^2} \tag{14}$$

with initial and boundary conditions

$$T(r, 0) = T_{\text{sat}}, \quad T(a, t) = T_c, \quad T(r_s, t) = T_{\text{sat}} \tag{15}$$

In Eq. (15) r_s is unknown, so an additional equation is required. A heat balance at the surface of the condensate on the cooling tube provides the final condition that must be satisfied. From a mass balance in the vapor phase, mass flux is constant along r, including at the liquid-vapor interface (i.e., the condensate surface). Conduction through the vapor phase is zero. The heat balance then reduces to

$$k_l \frac{\partial T}{\partial r}\bigg|_{r=r_s(t)} = \rho_l h_{fg}\frac{dr_s}{dt} \tag{16}$$

The mathematical model of the cylindrical system is thus reduced to a one-dimensional conduction heat-transfer problem with a moving boundary condition.

Fill takes place by the displacement of the condensed vapor by the bulk liquid, which moves into the channel through the screen wall. A mass balance on a control volume around the vapor region provides the relationship between the radius of the bulk and condensate liquid-vapor interfaces that bound the vapor region:

$$r_b = \left(r_{b0}^2 - \frac{\rho_l - \rho_v}{\rho_v}\left(r_s^2 - a^2\right)\right)^{\frac{1}{2}} \tag{17}$$

Equations (14) through (17) represent a complete model of filling a cylindrical channel with a concentric cooling tube. Equations (14) through (16), which provide the condensate surface radius, represent the general problem of one-dimensional cylindrical conduction with a moving change-of-phase boundary. Equation (17) provides the corresponding radius of the opposing bulk liquid surface.

Before the solution is addressed, consider the apex-mounted heat-exchanger configuration. This configuration poses a more complex environment for the fill process in low gravity, because liquid configurations are more complex. A model that provided for all liquid geometries at all times would necessarily be very complex, involving surface tension, momentum, and convection and conduction heat transfer. In the present analysis, the interfaces are approximated as flat and parallel. The approximation is reasonable for early times, but probably not realistic for later times when substantial quantities of liquid have entered the channel. It does not take into account the effect of convection from coalescence of condensate and bulk liquid surfaces or the subsequently enhanced thickness of liquid near the heat exchanger. However, the model still can provide an order of magnitude for the time to fill the triangular channel and provide a basis for insight into the time it takes to fill the channel. The effect of the approximation is to reduce the set of governing equations to exactly those of the concentric heat-exchanger configuration.[4] Thus, Eqs. (14–17) provide a representation of the filling of both the cylindrical and the triangular apex-mounted configurations.

Two types of solutions to Eqs. (14–17), particularly the heat-transfer problem of Eqs. (14–16), will be considered below. The first entails a simplifying quasi-steady assumption that allows analytical solution. The second is a numerical solution to the full transient problem.

Analytical Solution

No closed-form analytical solution to the problem of cylindrical one-dimensional conduction with moving phase boundary has been found. An approximate solution that uses a series expansion as applied to freezing of water on a pipe is provided in Ref. 8.

An approximation that allows for a closed-form solution is to assume that the temperature profile at any given time is the steady-state profile that would be reached if the outer boundary were fixed at the location corresponding to the given time. The solution, referred to as the quasi-steady-state solution, is found in Ref. 9 and corresponds to the zeroth-order solution in Ref. 8, which showed that it is a very good approximation for the problem of ice formation. That the neglect of the transient term is a reasonable assumption for hydrogen is revealed by nondimensionalizing the governing Eqs. (14–16), yielding

$$Ja\frac{\partial\theta}{\partial\tau} = \frac{1}{\eta}\frac{\partial\theta}{\partial\eta} + \frac{\partial^2\theta}{\partial\eta^2} \tag{18}$$

$$\theta(\eta, 0) = 1, \qquad \theta(1, \tau) = 0, \qquad \theta(\gamma, \tau) = 1 \tag{19}$$

$$\frac{\partial\theta}{\partial\eta}\bigg|_{\eta=\gamma(\tau)} = \frac{d\gamma}{d\tau} \tag{20}$$

For $Ja \ll 1$, the transient term in Eq. (18) is neglected, leaving

$$0 \approx \frac{1}{\eta}\frac{\partial\theta}{\partial\eta} + \frac{\partial^2\theta}{\partial\eta^2} \tag{21}$$

Equations (19–21) represent the system to be solved for the quasi-steady solution. Equation (21) is solved for the (nondimensional) temperature profile using the boundary conditions in Eq. (19); the resulting steady-state temperature profile is substituted into Eq. (20), producing an implicit relation for the nondimensional condensate coordinate $\gamma(\tau)$, which is equivalent to that found in Ref. 9:

$$\tau = \gamma^2 \ln\frac{\gamma}{2} - \frac{\gamma^2}{4} + \frac{1}{4} \tag{22}$$

Finite-Difference Solution

Returning to Eqs. (14) through (16), the full transient problem is solved numerically by finite-differencing. To facilitate the finite-difference solution, a different nondimensional radial coordinate, ζ, is used, transforming Eqs. (14–16) into

$$\frac{\partial\theta}{\partial\tau} = \frac{a^2}{Ja}\left\{\left[\frac{(Ja/a^2)\zeta}{r_s(\tau) - a}\frac{dr_s(\tau)}{d\tau} + \frac{1}{\{[r_s(\tau) - a]\zeta + a\}(r_s(\tau) - a)}\right]\frac{\partial\theta}{\partial\zeta} + \frac{1}{[r_s(\tau) - a]^2}\frac{\partial^2\theta}{\partial\zeta^2}\right\} \tag{23}$$

$$\theta(\zeta, 0) = 1, \qquad \theta(0, \tau) = 0, \qquad \theta(1, \tau) = 1 \tag{24}$$

$$\frac{\partial\theta}{\partial\zeta}\bigg|_{\zeta=1} = \frac{r_s(\tau) - a}{a^2}\frac{dr_s}{d\tau} \tag{25}$$

Notice that the surface temperature gradient is now always evaluated at a fixed point, namely $\zeta = 1$. An alternative form of Eq. (25) is

$$\frac{d[r_s(\tau) - a]^2}{d\tau} = 2a^2\frac{\partial\theta}{\partial\tau}\bigg|_{\zeta=1} \tag{25a}$$

Central differencing of the spatial variables and fully implicit differencing of the time derivative in Eq. (25) yields a finite-difference equation for the temperature for each radial node. (The node equation is defined in the Appendix.) The resulting system is solved for the temperature profile using the tridiagonal matrix algorithm. The solution proceeds from the known initial conditions to a new time by guessing the new $r_s(\tau)$. From the corresponding temperature profile the temperature gradient at $r_s(\tau)$ is evaluated using simple

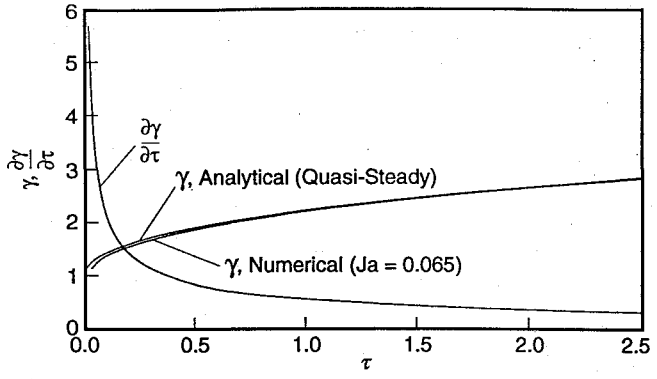

Fig. 3 Predicted growth of condensate liquid layer in time.

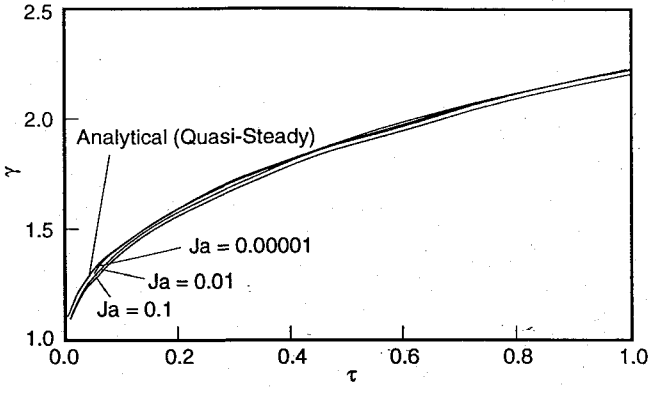

Fig. 4 Comparison of predicted nondimensional growth rate of condensate layer for different *Ja*.

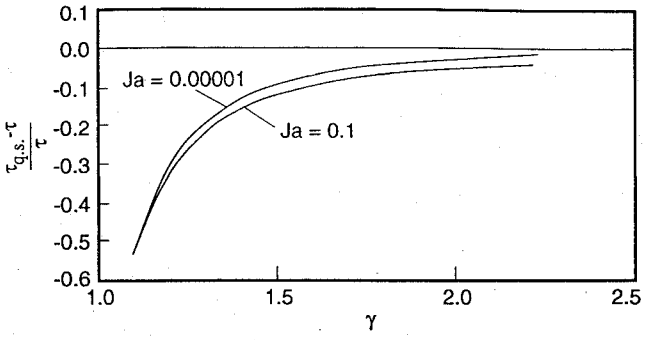

Fig. 5 Difference between the growth times predicted by the transient and quasi-steady solutions decreases with growth of the condensate layer.

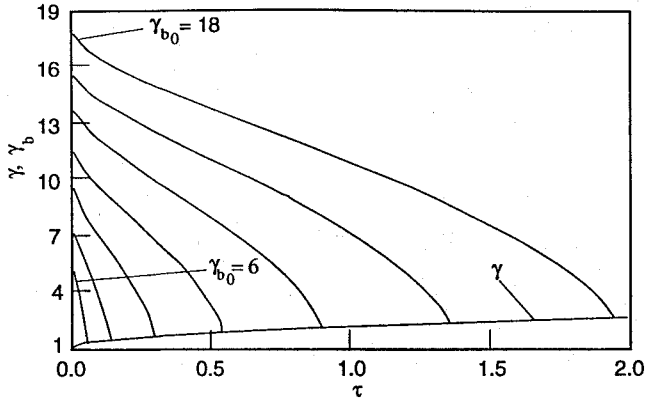

Fig. 6 Predicted bulk-liquid and condensate-layer locations with time for use in design analysis.

backward spatial differencing. Then from the interfacial condition, Eq. (25a), in finite-difference form, we have

$$\frac{\mathrm{d}[r_s(\tau)-a]^2}{\mathrm{d}\tau} = 2a^2\frac{\theta_N-\theta_{N-1}}{\Delta\zeta} \tag{26}$$

Note that the system of equations is now fully implicit and robust against numerical instabilities.

A guess of $r_s(\tau)$ for each new time step is provided by linear approximation of surface growth by Taylor expansion in time,

$$(r_s-a)^{2^{(\nu+1)}} \approx (r_s-a)^{2^{(\nu)}} + \frac{\mathrm{d}(r_s-a)^2}{\mathrm{d}\tau}\Delta\tau \tag{27}$$

Relaxation then provides a quick path to convergence on $r_s(\tau)$ for time τ. Solution proceeds simply by marching forward in time. Ten grid points were ample for grid independence, and after the first time step, only two iterations were required for convergence to within 1%.

Theoretical Results and Discussion

Plots of the growing condensate-layer coordinate over time as obtained from the quasi-steady-state analytical solution and the finite-difference solution (for $Ja = 0.065$) are shown in Fig. 3. Both results show that the rate of growth of the condensate layer starts large when the cooling tube is bare, but drops off asymptotically toward zero as the layer thickens. Figure 3 also indicates that the analytical solution using the quasi-steady assumption, equivalent to $Ja = 0$, is a good approximation of the case of the particular Jakob number plotted.

The surface-radius solutions are plotted for a wider range of Jakob numbers in Fig. 4. All of the plots indicate that the quasi-steady assumption, reflected by the analytical solution, is a good one for Jakob numbers considered. Also, the smaller the Jakob number, the closer the results are to the analytical solution. This result supports the dimensional analysis that leads to the quasi-steady assumption; i.e., for Jakob numbers approaching zero in Eq. (18) the transient temperature term may be neglected, so that we have Eq. (21). The location of the curves for positive Ja below that of the quasi-steady solution is due to the resistance of real fluids to temperature change (positive c_p), which serves to slow down transients to the steady-state solution and thus condensation and surface growth.

Plots of the difference between the transient numerical solution and the quasi-steady analytical solution for two Jakob numbers are shown in Fig. 5. This figure bears out the trend that the transient solution approaches the quasi-steady solution asymptotically as the condensate layer grows. Physically, this means that the liquid temperatures near the liquid-vapor interface (i.e., condensate surface) quickly approach the saturation temperature as the interface moves away from the cold sink of the cooling wall for this geometry.

The significance of the above results is that the contribution of the transient term to the solution is very low, and by using the nondimensionalized time τ, condensate-layer growth can be well approximated by one curve, the implicit analytical quasi-steady solution, Eq. (22), for the range of Jakob numbers considered. An explicit relation for the surface radius at any given time is provided by a third-order curve fit of the numerical data plotted in Fig. 4, for $0.00001 < Ja < 0.1$,

$$\gamma = 1.172 + 1.874\tau - 1.079\tau^2 + 0.263\tau^3 \tag{28}$$

Channel fill times are then determined using Eq. (28) in conjunction with the solution for the bulk surface position Eq. (17), which in nondimensional terms is

$$\gamma_b = \left(\gamma_{b0} - \frac{\rho_l-\rho_v}{\rho_v}(\gamma^2-1)\right)^{\frac{1}{2}} \tag{29}$$

Figure 6 summarizes the results for a range of channel-to-heat-exchanger diameter ratios. The initial bulk liquid surface location, γ_{b0}, is equated to the corresponding channel diameter. Therefore, smaller values of γ_{b0} correspond to smaller volumes of vapor that must be displaced. The intersections of the plots of bulk surface radius with the condensate-layer interface line represent full channels, i.e., the total time to fill the channels. From this figure any one

of the fill time, Ja (the temperature drop), and the channel-to-heat-exchanger diameter ratio can be found upon selecting the values desired for the other two. As an example, consider the scenario in which half an hour is prescribed as the maximum time available to fill a channel under the baseline environment and an initial system trade limits the temperature drop across the Joule-Thomson valve to 4 K ($Ja = 0.086$). Using Fig. 6 or Eqs. (28) and (29), it is found that a channel-to-heat-exchanger diameter ratio of 5 is required. This corresponds to a 17-mm-diam TVS tube, a reasonable size.

Proof-of-Concept Testing

Tests at $1g$ were performed to prove the feasibility of the proposed concept. The pivotal feature of the concept is that a temperature difference can effectively drive the filling of the channel. The primary test requirement is therefore to insure that the temperature difference is the sole driver for the fill process. The approach is to observe visually the filling of a channel with a reference test fluid and similar Jakob numbers.

Test Setup

A schematic of the test apparatus and setup is shown in Fig. 7. The test apparatus was divided into five functional groups: the test article, test tank, liquid supply and storage, TVS, and instrumentation and support equipment.

The test article was a segment of LAD channel integrated with a TVS heat exchanger. The design of the test article is shown in Fig. 8, and a photograph is shown in Fig. 9. The channel was 33 cm long and had a triangular cross section (5.1-cm and 6.3-cm inside height and base, respectively). The TVS cooling tube was at the apex of the channel; with this design, bulk liquid had to move upward against gravity toward the cooling tube. Consequently, gravity was

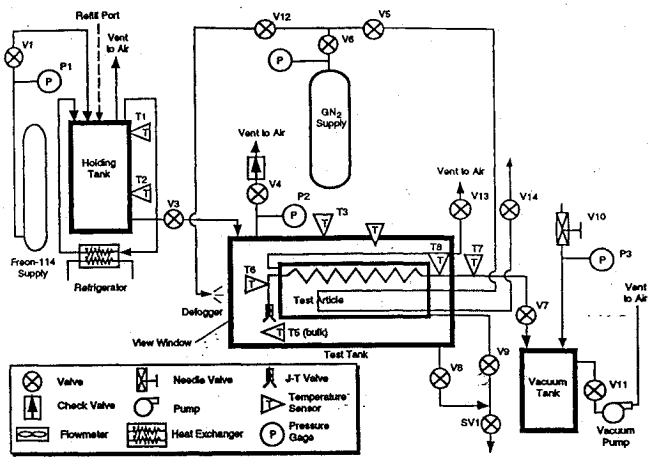

Fig. 7 Test-setup schematic.

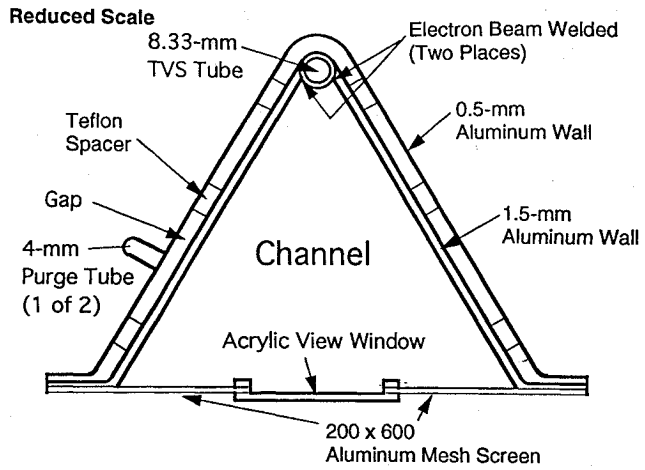

Fig. 8 Design drawing for apex-mounted heat exchanger, 1 g test article (cross-sectional axial view).

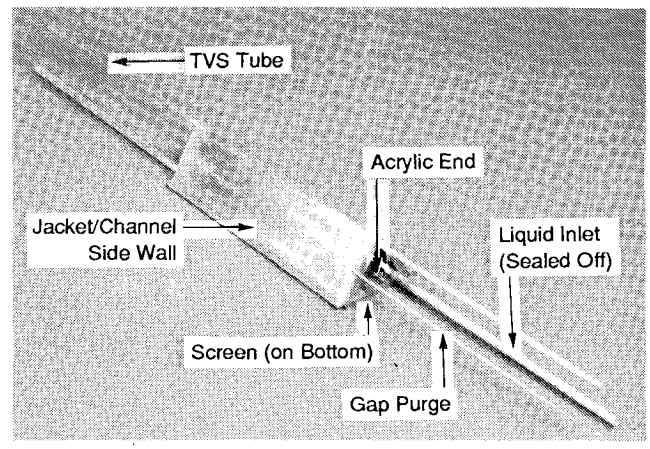

Fig. 9 Photograph of apex-mounted heat exchanger, 1 g test article.

effectively eliminated as a driver for channel fill and actually worked against fill. One end of the channel was transparent acrylic (shown in the photograph) to allow observation of the contents of the channel. The bottom of the triangular channel included the screen surface, which extended from one end of the channel to the other. Each side of the triangular channel was actually a double wall with a gap. The gap was tapped by two 3.2-mm tubes to allow purging of the gap with a low-conductivity gas or evacuation of the gap; a nitrogen purge was used in this test effort. (The double wall and purge option improved thermal insulation of the TVS cooling tube and the internal channel side walls in an operational environment.)

The test tank housed the test article. The test tank was cylindrical, 20 cm in internal diameter and 46 cm long, and was sized to be as small as possible to save liquid costs, but large enough to provide room for the test article and plumbing and so that the bulk liquid level did not vary significantly during the course of a LAD fill test. The transparent polycarbonate end plates of the tank allowed for a view of the LAD channel and bulk liquid. A thin mat of rubber between the polycarbonate and steel flange provided a liquid seal for each end. The cylindrical portion of the test tank was insulated with 2.5 cm of foam wrap. The edges (flange portion) of the end plates were insulated using split pipe-foam insulation. One of the polycarbonate windows (front end of the tank) was left clear for primary view of the fill process. This window was blown on its external side with dry gaseous nitrogen (using a pressurized cylinder source) to keep it dry of condensing water vapor. The other (back) polycarbonate end provided for penetrations for most of the tank plumbing.

The test fluid was Freon-114; it allowed for the desired Jakob numbers (on the order of 0.1) at reasonable pressure drops, and because of its normal boiling point of 277 K and safe characteristics, it was a convenient test fluid. Tank bulk liquid was supplied by the holding-tank feedline, which penetrated the top of the test-tank cylinder. The test-tank bulk liquid drain was located on the bottom of the test tank toward the back. The bulk ullage environment of the tank was vented through a vent near the high point of the tank and discharged into the lab.

The TVS Joule-Thomson (J-T) valve was a Lee Viscojet (500D rated at 5000 Lohm).[10] The J-T valve was sized to promote sustained two-phase flow along the cooling tube by increasing the cooling capacity (note, however, that two-phase flow was apparently not maintained during the testing). The J-T valve was mounted 5 cm upstream of the channel. The inlet to the TVS was simply the open end of a short piece of tubing attached to the upstream side of the J-T valve. TVS backpressure control was provided by a vacuum tank that was evacuated by a standard centrifugal pump. The vacuum tank was sized so that manual adjustment of a needle valve was sufficient to maintain a constant backpressure.

Test Procedure

The test procedure included four principal steps: 1) purge of the LAD wall gap, 2) fill of the test tank, including purge and setting of the liquid level, 3) setting of the TVS backpressure, and 4) LAD fill.

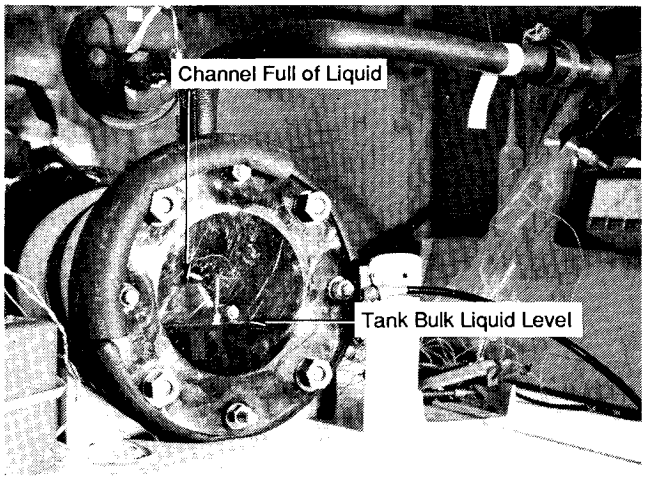

Fig. 10 Test setup for fill of channel (test 8).

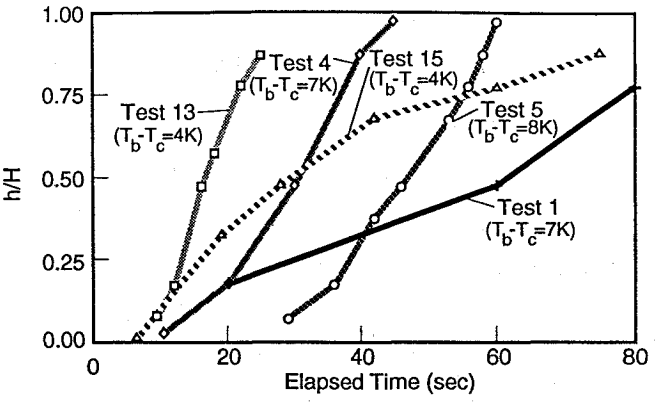

Fig. 11 Observed height-ratio time traces for high-fill-ratio tests.

The wall gap of the LAD was purged with dry nitrogen by opening the gap purge inlet and outlet valves and then briefly cracking the nitrogen source. The purge outlet was simply checked for positive flow of gas, and the source and inlet and outlet valves were then closed.

The test tank was then filled by opening the feedline valve with the test-tank vent open. The test-tank fill continued until liquid reached the vent valve and actually spilled overboard through the valve to insure that all gases, including noncondensibles, were expelled.

After the test tank was filled, the test-tank vent was closed and the bulk-liquid outlet and LAD liquid outlet were opened. Subsequent heat leak into the tank resulted in pressurization of the test tank (to a fraction of a psi) and allowed liquid to be expelled from the tank. The bulk-liquid level was set to a height just above the bottom of the front end of the LAD channel. At this height, all screen surface was submerged, as is required for the LAD fill process to work, but the channel was mostly empty of liquid. The tank vent was then reopened to maintain constant ullage pressure at ambient pressure.

The vacuum pump was turned on while the TVS heat-exchanger outlet was still closed. The needle valve was then opened until the desired backpressure was reached. The TVS was started by opening the TVS heat-exchanger outlet valve, which established the desired pressure difference across the J-T valve. The backpressure was monitored and adjusted if necessary (usually a quick adjustment at the start of the test was required, and only minor adjustments were necessary subsequently during the fill). The temperature data were recorded manually; only a gross correlation of temperatures with time could be achieved. The liquid level inside the test article LAD channel was monitored and recorded on video to evaluate the effectiveness of fill. When the test article was filled with liquid, or if fill was clearly not forthcoming, the TVS heat-exchanger outlet valve was closed to terminate the TVS flow. The test article was observed for a short time following flow termination to evaluate the postflow behavior of the fluid inside the test article.

Each test was performed at one pressure drop; most were performed at one of three principal values: 0.07, 0.05, and 0.03 MPa. The 0.05-MPa pressure drop corresponds to a Jakob number of 0.07, which is representative of the application of the concept in a servicing environment. The relative success of each test is characterized by the visually observed peak fill level, which is quantified by the fill height ratio, h/H. (Note: the epoxied plumbing exiting the channel window obscured the view at the apex; complete fill could not be directly observed.)

Experimental Results and Discussion

There were a total of sixteen tests performed in six test sessions. Details of the tests are reported in Ref. 4. Six of the tests resulted in substantial fill of the channel, i.e., $\geq$ 0.9 fill ratio. Two of the tests resulted in complete fill as far as could be observed. Figure 10 shows the test article full of liquid at the end of one of the tests and the tank fill level just above the base of the channel.

Two principal processes worked against all of the fills: 1) heat leaks into the channel, and 2) the leak of noncondensible nitrogen gas from the nitrogen-purged gap into the channel. The heat leaks were primarily from 1) conduction through the LAD plumbing that penetrated the tank and 2) condensation at the J-T valve. The conduction through the LAD plumbing was evidenced by bubbles emanating from the inlet to the LAD outlet, which is located near the base of the channel just inside of the channel window. This increased the amount of vapor that had to be condensed for any given fill and slowed the fills. The conductive heat through the plumbing penetrations was reduced after test 3, when a segment of Tygon tubing was inserted in the line before V9. The condensation at the J-T valve was evidenced by the dripping of liquid from the J-T valve. The leak of noncondensibles is the reason proposed for virtually all of the incomplete fills. These gases served to inhibit the condensation process at the TVS heat exchanger (cooling tube), eventually stopping it altogether as its concentration increased with either higher fill level or continued leak into the channel. It is believed that the noncondensible leakage was continuous, as promptness in starting a fill appeared to result in a faster fill, whereas long delays appeared to result in a substantially slower fill. Leaks also resulted in the eventual reversal of fill following the stall of a fill at its peak value that was observed in the tests where extended observations were made. A path for leakage was substantiated when liquid was observed exiting the LAD wall gap purge line during preparation for test 13.

The fill traces for five of the tests that resulted in substantial fill are shown in Fig. 11 (no temperature trace was available for the sixth test). Under ideal conditions, one would expect test 5 to have resulted in the fastest fill. However, test 13, which had one of the lowest temperature differences, was the fastest.

The low-gravity analysis described above does not apply to the $1g$ test configuration. So to assist in evaluation of the test results, we used a simplified steady-state analytical model. In the model, the channel was approximated as two symmetric, thin, long, rectangular-cross-section fins with infinite depth, each with constant temperature at the cooling-tube end and zero gradient at the other. The vapor inside of the channel was assumed constant at the saturation temperature of the bulk liquid. A falling film-condensation heat-transfer coefficient, adjusted for the angle of the fins, was used for the heat transfer from the channel vapor to the fins. Heat transfer on the outside of the fins was comparatively small and approximated as adiabatic. Progression of the fill was assumed quasi-steady. During each time step, all heat going into the fin was assumed to be from condensation of the vapor inside the channel. As the vapor condensed, the liquid filled the channel from the bottom up and the area of the fin was adjusted accordingly for subsequent time steps. Further discussion on the model, including the classical fin solution and how it was used, is available in Ref. 4.

In Fig. 12 the fill trace for test 13 is compared with corresponding calculations from the fin model. The calculated values are shifted to start when the actual start of fill was observed. This shift compensates for some of the transient conditions associated with cooling the hardware, which the steady-state model does not itself take into

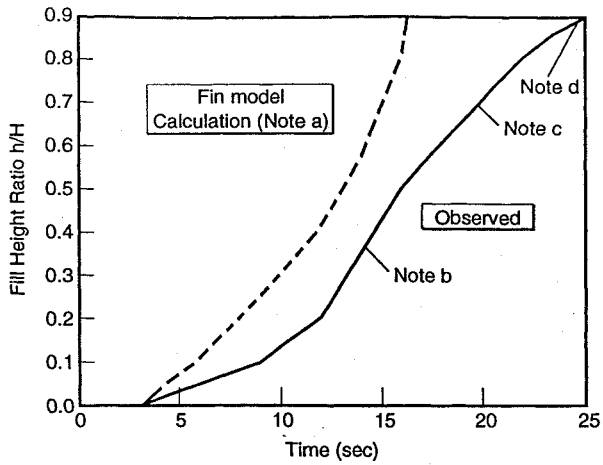

a. Using quasi-steady fin model with J-T valve inlet (bulk) temperature (278 K) and average TVS temperture (274 K)
b. Fill profile lowered due to transients and heat leak
c. Fill profile flattened due to presence of noncondensibles in LAD channel
d. Highest verifiable fill ratio was 0.9 due to obstructed view of uppermost portion of channel

Fig. 12 Comparision of test-13 results with steady-state fin-model calculations.

account. The leak of heat and that of noncondensible gas into the channel both cause the observed fill level to fall below the calculations. The flattening of the observed fill line toward the end of fill is attributed to the increase in concentration of noncondensibles, which is due to diminishing vapor mass and continued leak of noncondensibles. Test 13 was performed with the fastest turnaround from fill of the test tank to start of the TVS; consequently, there was less time for noncondensibles to leak into the channel, allowing for a faster fill once the TVS was started. In summary, the nonideal test conditions resulted in large variations in fill conditions and fill times, and thus to the lack of discernible trends in Fig. 11.

Conclusions

The low-gravity performance analysis and the proof-of-concept testing together show that the proposed concept of filling screen-channel liquid acquisition devices in low gravity by cooling them, using a thermodynamic vent system, is not only viable but very promising. The basis of the concept is that actively cooling a channel and its contents enhances condensation and Clapeyron pumping, which drive the fill of the channel.

The low-gravity analysis effort reduced the prediction of performance under various sizes and temperatures to a very simple set of equations for use in prediction of fill performance in hydrogen. The numerical results verified that the quasi-steady analytical solution is appropriate for consideration in hydrogen storage systems. The results can be a very useful tool in system trades, as the required channel size and fill times can be defined for a specified limitation on the thermodynamic vent flow (i.e., temperature or J-T expansion, and flow rate). Reasonable fill times with reasonable channel and heat-exchanger sizes are predicted in the baseline environment.

The tests convincingly prove the feasibility of the concept, as the apex-mounted configuration test article was successfully filled in Freon-114 against $1g$. The testing could not be used to validate any expected trends in the fill process, because of significant apparent leakage of fill-inhibiting noncondensibles into the test-article channel.

The results of this effort indicate that the concept is ready for low-gravity testing. Testing on a KC-135 should be adequate for validation of the analysis, because fill times well within the 20 s of low gravity, available during KC-135 tests, can be achieved.

Appendix: The Node Equation

The finite-difference equation for temperature for each radial node is

$$\theta_n^{(v+1)} = a_n\theta_{n+1}^{(v+1)} + b_n\theta_{n-1}^{(v+1)} + c_n \tag{A1}$$

where

$$a_n \equiv \left(\frac{\Delta\tau Q(\tau)}{\Delta\zeta^2} + \frac{\Delta\tau P(\zeta,\tau)}{2\Delta\zeta}\right) \Big/ \left(\frac{2\Delta\tau Q(\tau)}{\Delta\zeta^2} + 1\right) \tag{A2}$$

$$b_n \equiv \left(\frac{\Delta\tau Q(\tau)}{\Delta\zeta^2} - \frac{\Delta\tau P(\zeta,\tau)}{2\Delta\zeta}\right) \Big/ \left(\frac{2\Delta\tau Q(\tau)}{\Delta\zeta^2} + 1\right) \tag{A3}$$

$$c_n \equiv \theta_n^{(v)} \Big/ \left(\frac{2\Delta\tau Q(\tau)}{\Delta\zeta^2} + 1\right) \tag{A4}$$

$$P(\zeta,\tau) \equiv \left(\frac{\zeta}{r_s(\tau) - a}\frac{\mathrm{d}r_s(\tau)}{\mathrm{d}\tau} + \frac{a^2/Ja}{\{[r_s(\tau) - a]\zeta + a\}[r_S(\tau) - a]}\right) \tag{A5}$$

$$Q(\tau) \equiv \frac{a^2/Ja}{[r_s(\tau) - a]^2} \tag{A6}$$

with boundary temperature conditions

$$\theta_1 = \theta_c = 0 \tag{A7}$$

$$\theta_N = \theta_{\text{sat}} = 1 \tag{A8}$$

References

[1]Rybak, S. C., Willen, G. S., Follett, W. H., Hanna, G. J., Cady, E. C., DiStefano, E., and Meserole, J. S., "Feasibility Study for a Cryogenic On-Orbit Liquid Depot-Storage, Acquisition and Transfer (COLD-SAT) Satellite," Final Report for Phase A Study, NASA CR-185248, Aug. 1990.

[2]Smith, J. M., and Van Ness, H. C., *Introduction to Chemical Engineering Thermodynamics*, 3rd ed., McGraw-Hill, New York, 1975, p. 185.

[3]Florshuetz, L. W., and Chao, B. T., "On the Mechanics of Vapor Bubble Collapse," *Journal of Heat Transfer*, Vol. 87, May 1965, pp. 209–220.

[4]DiStefano, E., "Fill of Screen Liquid Acquisition Devices in Low Gravity Using a Thermodynamic Vent System," M.S. Thesis, Univ. of California, Irvine, CA, Jan. 1991.

[5]Plesset, M. S., and Zwick, S. A., "A Non-steady Heat Diffusion Problem with Spherical Symmetry," *Journal of Applied Physics*, Vol. 23, Jan. 1952, pp. 95–98.

[6]Kosson, R., Hembach, R., Edelstein, F., and Tawil, M., "A Tunnell Wick 100,000 W-in. Heat Pipe," AIAA Paper 72-273, Apr. 1972.

[7]Symons, E. P., "Wicking of Liquids in Screens," NASA TN D-7657, May 1974.

[8]Pekeris, C. L., and Slichter, L. B., "Problem of Ice Formation," *Journal of Applied Physics*, Vol. 10, Feb. 1939, pp. 135–137.

[9]Carslaw, H. S., and Jaeger, J. C., *Conduction of Heat in Solids*, 2nd ed., Oxford Univ. Press, London, 1959, p. 296.

[10]Anon., *Technical Hydraulic Handbook*, 8th ed., Lee Co. Technical Center, Westbrook, CT, 1987, p. 147.